RIGID BODY MODEL OF THE HYBRID III DUMMY LOWER LIMB INCLUDING MUSCLE TENSION UNDER CAR CRASH CONDITIONS

Philippe PETIT*, Laurent PORTIER**, Xavier TROSSEILLE***

* CEESAR
132, rue des Suisses, 92000 Nanterre - FRANCE.

** TEUCHOS
6 avenue du Général De Gaulle, 78000 Versailles - FRANCE.

*** Biomedical Research Department - RENAULT S.A
132, rue des Suisses, 92000 Nanterre - FRANCE.

ABSTRACT :

As of today, neither human surrogates such as crash test dummies and cadavers, nor mathematical models can take lower limb bracing into account. It is however reported that more than 50% of car drivers have time to anticipate an impending crash.

Based on an in-depth literature review, a mathematical representation of muscle tension was adapted from gait conditions to car crash conditions using available animal experiment results.

This mathematical representation uses 3 generic functions associated with 3 specific parameters to describe muscle mechanical responses.

Meanwhile, the human muscle/skeleton geometry of lower extremities was scaled to correspond to the thigh and leg lengths of the 50th percentile Hybrid III dummy model available in Pamsafe software.

For the model development, muscle paths were imposed using origins, insertions and a variable number of pulleys, in order to obtain proper muscle moment arms relative to the different joints whatever the position of the dummy.

A particular attention was paid to the knee extensors and to the patella.

The entire lower limb musculature was modeled using 18 equivalent muscles per limb, including both agonist and antagonist muscles responsible for the application of a load on a brake pedal or a foot-rest.

Dynamic cadaver experiments and volunteer tests were used both to determine the muscle activation coefficient set and to validate the contributions of passive and active muscle forces of the model.

Simulations show that muscle tension can significantly modify the dummy kinematics during a crash.

AS OF TODAY, NEITHER HUMAN surrogates such as crash test dummies and cadavers, nor mathematical models can take lower limb bracing into account. It is, however, reported that more than 50% of car drivers have time to anticipate an impending crash [26]. It means that the driver's hip, knee and foot extensors are fully activated when the crash occurs. Moreover, Portier [23] reported that during a dynamic dorsiflexion imposed to the foot of a cadaver, the tensile force in the Achilles tendon could reach 1.9 kN due to the passive influence of plantarflexion muscles. An active force of 5.3 kN measured in the Achilles tendon was reported by Grafe [12] during acrobatic jumps. Keeping in mind that the foot over range of motion dorsiflexion was clearly identified as one of the ankle injury mechanism, both active and passive muscle tensions could have a protective effect on the ankle joint.

Since it is not possible to perform volunteer tests under severity conditions comparable to real world accidents, a new method was developed to set up a simplified lower extremity musculature on a mathematical articulated rigid body model of the 50th percentile Hybrid III. The actual objective is to study the influence of muscle tension on both the occupant kinematics and the loads passing through the lower limbs. The entire work was based on geometrical and physical data available in the literature for either human being or animals.

EQUIVALENT MUSCLES

In the literature, methods such as the « quick release » or the « controlled release », initially used in isolated animal muscular preparations were adapted to measure human in-vivo muscular characteristics [11].

Other authors assessed the visco-elastic properties of systems composed of muscles surrounding a single joint, using either the natural frequency of the free oscillations [9], or the frequency response of either stochastic [16] [17] or harmonic [1] [2] applied oscillations.

All the in-vivo methods are based on the 4 following assumptions :

- the different segments are considered as articulated rigid bodies,
- the joint centers of rotation are fixed (hinge, spherical and universal joints),
- the problem of distinguishing between individual muscles is avoided by assuming that a single equivalent muscle acts to flex or extend a particular joint.
- the latter implicitly assumes first that the action of the antagonists is either negligible or modeled separately, second that the ratio between the moment produced by a particular muscle of the group and the total moment produced by the group is constant all over the range of motion.

When listing the main muscles involved in lower limb bracing and their antagonists, they correspond to the muscles involved in gait. This remark provides many musculoskeletal results available in the literature from the physiological gait investigation studies.

One regroupment that satisfies the assumptions above and contains the muscles of our interest is proposed by Hoy [15]. Table 4 gives the equivalent muscles and their actions relative to the lower limb joints.

MUSCULOSKELETAL GEOMETRY

THE DATA CONCERNING MUSCLE ORIGINS AND INSERTIONS are mainly based on the study performed by White [27]. In that study, the authors have identified and located the origins and insertions of 40 lower limb muscles from dry bones of a human cadaver.

White reported all the coordinates in local frames. The thigh, calf and pelvis dimensions of the cadaver did not correspond to the distances between the centers of rotation of the 50th percentile Hybrid III dummy. That is the reason why some geometrical transformations were applied to the cadaver data. The pelvis was transversally scaled using the distance between the two hip sockets. Femur and tibia/fibula scalings were also performed using the distances between the hip, knee and ankle joint centers of rotation. Table 1 reports the scaling ratios.

Distances	Cadav. White (m)	HIII Pamsafe (m)	Scaling ratio
CR left hip - right hip	0.173	0.170	0.983
CR hip - knee	0.465	0.400	0.859
CR knee - ankle	0.387	0.413	1.067

Table 1 : CR to CR distances and scaling ratios.

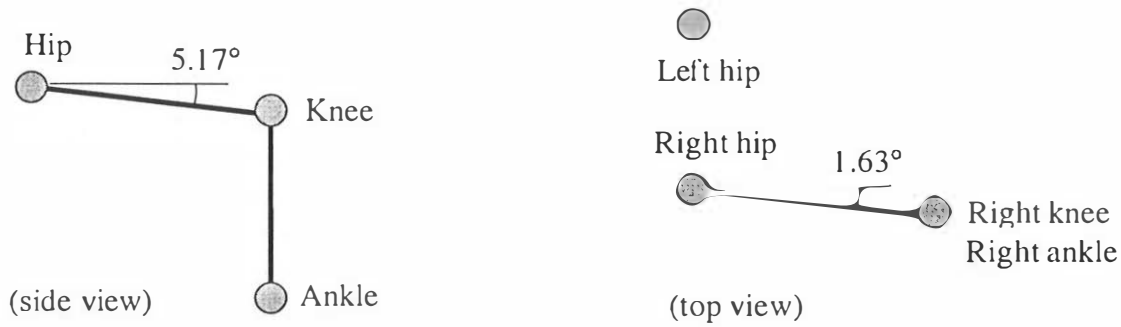

Figure 1 : Lower limb position of the Pamsafe 50th percentile HIII rigid body dummy model.

Once the origins and insertions of the 40 muscles were calculated in a global coordinate system for a dummy positioned as described in Figure 1, muscles were grouped. In case of spread origin or insertion, White reported the center of gravity of the origin or insertion area. The origin or insertion points of an equivalent muscle was defined as the center of gravity of the different origins or insertions the weightings of which were the muscle active cross section areas. The muscle active cross section areas used (Table 2) were those reported by Brand for a male specimen (37 years old, 1.83 m, 91 kg) and defined as the ratio between the muscle volume (measured by water displacement) and the average muscle fiber length.

Note : no active cross section area value was available for the biceps femoris long head and no geometrical information was reported for the origin and insertion of the peroneus tertius muscle. As a consequence, those two muscles were not taken into account to calculate the equivalent muscle origins and insertions although their mechanical contribution were included into the equivalent muscle total tensions.

Muscle	Active cross section areas (cm^2)	Muscle	Active cross section areas (cm^2)
Adductor brevis (Short head*)	11.52	Superior gemellus	2.13
Adductor brevis (Long head*)	5.34	Biceps femoris	27.34
Adductor longus	22.73	Gracilis	3.74
Adductor magnus (Anterior*)	25.52	Rectus femoris	42.96
Adductor magnus (Middle*)	18.35	Sartorius	2.9
Adductor magnus (Posterior*)	16.95	Semimembranosus	46.33
Gluteus maximus (Anterior*)	20.2	Semitendinosus	13.05
Gluteus maximus (Middle*)	19.59	Tensor fascia latae	8
Gluteus maximus (Posterior*)	20	Gastrocnemius (Medial*)	50.6
Gluteus medius (Anterior*)	25	Gastrocnemius (Lateral*)	14.3
Gluteus medius (Middle*)	16.21	Biceps femoris (Short head*)	8.14
Gluteus medius (Posterior*)	21.21	Vastus intermedius	82
Gluteus minimus (Anterior*)	6.76	Vastus lateralis	64.41
Gluteus minimus (Middle*)	8.2	Vastus medialis	66.87
Gluteus minimus (Posterior*)	11.98	Tibialis anteriosus	16.88
Iliacus	23.33	Extensor digit comm	7.46
Psoas	25.7	Extensor hallucis longus	6.49
Inferior gemellus	4.33	Flexor dig	6.4
Obturator externus	2.71	Flexor hall long	18.52
Obturator internus	9.07	Peroneus brevis	19.61
Pectineus	9.03	Peroneus longus	24.65
Piriformis	20.54	Peroneus tertius	4.14
Quadriceps femoris	21	Tibialis posterior	26.27
		Soleus	186.69

*Table 2 : Active cross section areas reported by Brand [8] for a male (37 years old, 1.83 m, 91 kg) and defined as the ratio between the muscle volume (measured by water displacement) and the average muscle fiber length (taking the fiber pennation angle into account). Note : the * indicates that the complete word was guessed from Brand's indications*

MUSCLE MOMENT ARMS relative to the joints they cross greatly depend on the occupant position and the muscle path. A variable number of pulleys were used for each muscle in order to ensure correct muscular moment arms relative to the hip, knee and ankle joints. The locations of the pulleys were determined from both anatomy papers and minute in-vivo examinations.

A particular attention was paid to the knee extension. Knee extensors insert on the patella, and the patella slides on the 2 femur condyles. A tendon connects the patella to the tibial anterior tuberosity. A solution involving an articulated rigid body was determined to model the patella. The positions of the muscle and tendon insertions and the location of the hinge joint connecting the patella and the femur were optimized in order to obtain a muscular moment arm (Figure 2) in agreement with the data reported from cadaver tests in the literature [25] [5] [20] [13]. Note : the knee extensor moment arm was defined as the ratio between the muscular tensile force and the moment created at the joint.

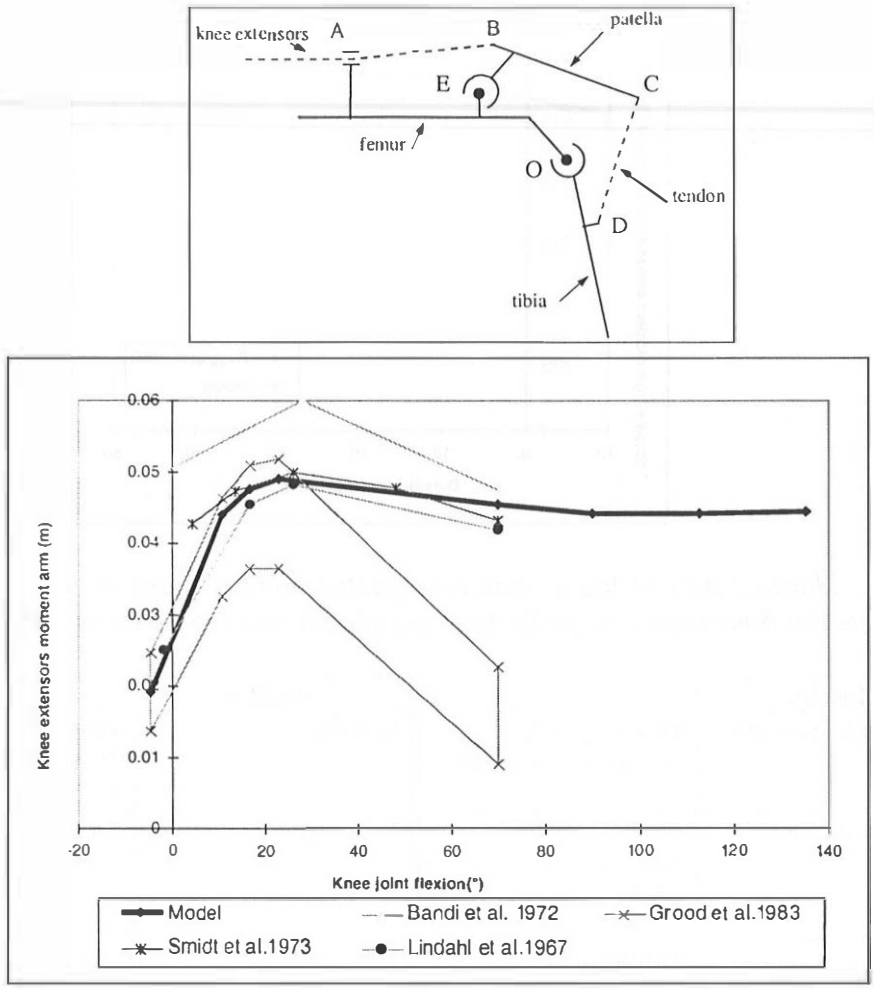

Figure 2 : sketch of the articulated rigid body solution used to model the patella and comparison of the moment arm obtained in that case and on cadaver versus knee angle.

The angular position of the patella relative to the femur is given by Equation 1. It is a polynomial approximation of the solutions determined in the resolution of the positions such that the distance CD (Figure 2) is constant all over the knee range of motion. The theoretical error due to the approximation is less than 1.1° for a total range of motion of 165° for the knee, and less than 0.2° for a knee flexion ranging from 60 to 120°.

$$\theta_{patella} = 6E\text{-}08\,\theta^{4}_{knee} + 2E\text{-}05\,\theta^{3}_{knee} + 0.0008\,\theta^{2}_{knee} + 0.6817\,\theta_{knee} - 0.0034$$

Equation 1 : angular position of the patella relative to the femur where θ_{knee} is the angle between the current knee flexion and the reference pamsafe position (Figure 1). $\theta_{patella}$ is the rotation angle to be applied to the patella from the reference position in order to have the proper length for the tendon inserted on the tibia. Note : angles are in radians.

The use of a pulley to impose the direction of the Achilles tendon at its insertion on the calcaneus provided a moment arm for the triceps surae in agreement with the data reported by Rugg [24] over the full ankle range of motion in flexion whatever the knee angle (Figure 3).

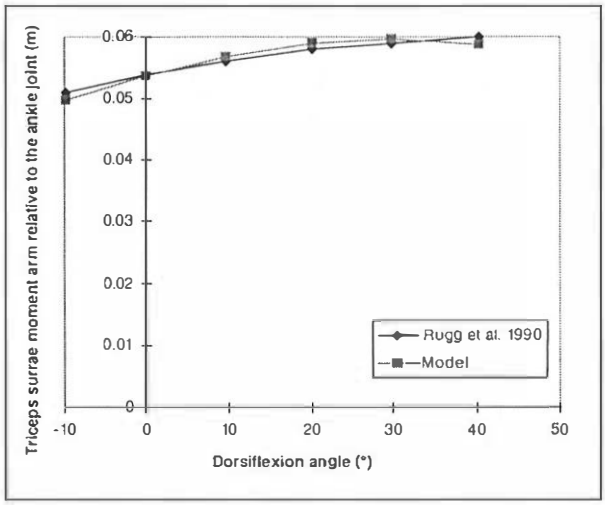

Figure 3 : Moment arm of the soleus and gastrocnemius muscles relative to the ankle joint versus the dorsiflexion angle for both our model and the cadaver [24].

Muscles		Muscles	
Adductor longus and brevis	Origin : pelvis Insertion : femur sup.	Gracilis	Origin : pelvis Pulley 1 : femur inf. Insertion : tibia sup.
Adductor magnus	Origin : pelvis Insertion : femur sup.	Sartorius	Origin : pelvis Pulley 1 : femur sup. Pulley 2 : femur inf. Insertion : tibia sup.
Rectus femoris	Origin : pelvis Pulley 1 : femur inf. Insertion : patella	« Hamstrings	Origin : pelvis Insertion : tibia sup.
Iliopsoas	Origin : pelvis Insertion : femur sup.	Biceps femoris (short head)	Origin : femur sup. Insertion : tibia sup.
Gluteus maximus	Origin : pelvis Insertion : femur sup.	Vasti	Origin : femur sup. Pulley 1 : femur inf. Insertion : patella
Gluteus medius	Origin : pelvis Insertion : femur sup.	Gastrocnemius	Origin : femur inf. Pulley 1 : tibia sup. Pulley 2 : tibia inf. Insertion : foot
Gluteus minimus	Origin : pelvis Insertion : femur sup.	Soleus	Origin : tibia sup. Pulley 1 : tibia inf. Insertion : foot
Pectineus	Origin : pelvis Insertion : femur sup.	Other plantarflexors	Origin : middle tibia Pulley 1 : tibia inf. Insertion : foot
Tensor fascia latae	Origin : pelvis Pulley 1 : femur sup. Insertion : tibia sup.	Dorsiflexors	Origin : middle tibia Pulley 1 : tibia inf. Insertion : foot

Table 3 : Description of the muscle paths. Note : on the Hybrid III dummy, a load cell is placed in the diaphysis, it defines the « femur sup. » and « femur inf. » portions as the proximal and distal parts respectively. « Tibia sup », « middle tibia » and « tibia inf » were defined similarly.

MUSCOLOTENDON ACTUATOR MODEL

Based on many works reported in the literature and more specially on Hoy [15] and Zajack [31] studies, the 18 equivalent muscles of each lower limb were modeled using 3 generic dimensionless functions and 3 specific parameters. The 3 generic dimensionless functions were the isometric active and passive forces vs muscle fiber length, and the force vs. shortening/strengthening velocity functions. They were normalized by the optimal muscle fiber length, the maximal isometric force and the maximal muscle fiber shortening velocity in order to obtain dimensionless relations. The 3 specific parameters were therefore the muscle optimal fiber length L_o^M defined as the fiber length at which the maximal isometric force can be generated, the maximal isometric force F_o^M, the maximal muscle fiber shortening velocity v_m.

STATIC PROPERTIES - When muscles were fully activated, we assumed that the isometric forces of any muscle could be determined using Equation 2. This implicitly assumed that the passive force starts for a muscle fiber length equal to the optimal fiber length.

$$\textit{Active: } (0.5 \le x \le 1.5) \quad \frac{F}{F_0{}^M} = -x^5 + 20.5x^4 - 71.75x^3 + 94.375x^2 - 50.5x + 9.375$$

$$\textit{Passive: } (1 \le x \le 1.5) \quad \frac{F}{F_0{}^M} = 41.146x^4 - 191.03x^3 + 335.77x^2 - 263.16x + 77.29$$

Equation 2 : Generic dimensionless functions giving the isometric active (for fully activated muscles) and passive forces where x represents the muscle fiber length normalized by the optimal fiber length L_o^M.

It is well established in the literature that the isometric active effort generated by a partially activated muscle equals the product of the active effort generated when fully activated by the activation coefficient *a*, i.e. $F(a<1)=a \cdot F(a=1)$.

DYNAMIC PROPERTIES - Myers [21] carried out dynamic experiments on isolated rabbit tibialis anterior. The results showed that the peak dynamic stretching effort did not depend on muscle activation and was approximately $1.9 * F_o^M$. Several authors claimed that the intersection of the curve with the abscissa axis remained unchanged whatever the activation. Moreover, since the intersection between the ordinate axis and the curve corresponds to an isometric force, we assumed that the force vs. shortening/lengthening velocity could simply be deduced from the fully activated muscle properties. Equation 3 finally gives the muscle isotonic dynamic properties as a function of normalized velocity and activation.

$$Shortening: x \le 0 : \frac{F}{F_0} = a.\left(\frac{1+x}{1-\frac{x}{\beta}}\right)$$

$$Lengthening: x \ge 0 : \frac{F}{F_0} = \frac{a + x.\frac{\eta}{\mu}}{1+\frac{x}{\mu}} - a$$

Equation 3 : muscular force - velocity generic dimensionless properties. a is the activation coefficient (ranging from 0 to 1), η is the ratio between the peak dynamic stretching force and the maximal isometric force, β and μ are 2 curve shape parameters chosen equal to 0.3 and 10.5 respectively in our study. x positive is the stretching velocity normalized by the maximal muscle fiber shortening velocity.

In agreement with many results reported in the literature, tendons were assumed to behave like linear springs, and to have a Young modulus equal to 1.2 10^6 Pa. Several authors [14] [18] [7] [3] showed that tendon characteristics were not sensitive to the lengthening velocity within the range of velocity caused by gait. We assumed this remained true under crash test conditions.

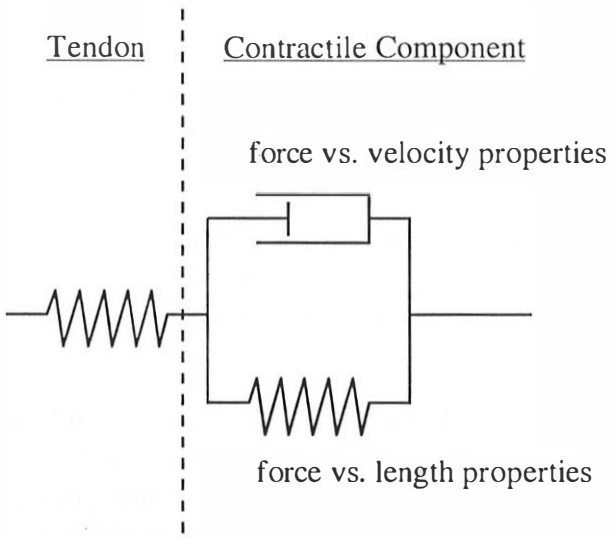

Figure 4 : Muscle model.

As presented in Figure 4, muscles were finally modeled using a linear spring (tendon) in series with a contractile component composed of a non linear damper (dynamic muscular properties - Equation 3) in parallel with a non linear spring (static passive and active muscular properties - Equation 2).

In agreement with literature results [6], we considered that the crash had such a short duration that the contractile component was unable to react. The muscular active effort versus time was thus assumed constant and equal to the initial active isometric force associated with the initial position of the dummy.

In the model we used (Figure 4) the initial muscular active force was represented by a pre-stressing of the elastic component (offset added to the force

vs. length curve).

Before a crash simulation, the dummy was positioned in the vehicle. For this particular position, the length of each muscle path was calculated using the origin, insertion and pulley coordinates. The length of the contractile component was then equal to the muscle path minus the length of the tendon (note : the latter did not depend on the position). From the length of the contractile component and the generic force vs. length muscular properties, an initial isometric active force was calculated, and the strain shift to be applied on the passive force vs. length curve was determined. The first 80-120 ms of simulation were used to reach an equilibrium position prior to the crash including active muscle tension.

MUSCULOTENDON PARAMETERS

The musculotendon parameters used were based on those reported by Hoy and determined by Wieckiewicz [28], and Brand [8]. To calculate each tendon length, we assumed that the peak moment generated at a joint was reached for a contractile component length equal to L_o^M. The joint angular positions corresponding to the maxima were determined from the moment curves reported by Hoy.

Muscle	Action	Fmax N	Activ. (<1)	Vm m/s	Lt m	Kt N/m	L_O^M m
Adductor longus and brevis	hip ext., hip flex.	838	0.75	1.32	0.050	785625	0.163
Adductor magnus	hip ext	1326	0.75	1.44	0.169	710357	0.154
Rectus femoris	hip flex, knee ext	926	1	0.82	0.294	84695	0.07
Iliopsoas	hip flex	1463	0.2	1.27	0.0	645441	0.158
Gluteus maximus	hip ext	1794	1	1.8	0.016	67275000	0.204
Gluteus medius	hip ext, hip flex	1849	0.9	0.81	0.033	1981071	0.089
Gluteus minimus	hip ext, hip flex	792	0.9	0.64	0.025	1188000	0.074
Pectineus	hip flex	212	0.2	1.3	0.0	7950000	0.162
Tensor fascia latae	hip flex, knee flex	239	0.2	1.18	0.436	20843	0.101
Gracilis	hip flex, knee flex	128	0.2	3.45	0.128	60000	0.446
Sartorius	hip flex, knee flex	124	1	5.66	0.0	116250	0.797
« Hamstrings »	hip ext, knee flex	2320	0.2	1.07	0.369	225974	0.091
Biceps femoris (short head)	knee flex	199	0.2	1.73	0.058	82917	0.187
Vasti	knee ext	5385	1	0.84	0.192	897500	0.072
Gastrocnemius	knee flex, plantarflexion	2293	1	0.48	0.406	202324	0.15
Soleus	plantarflex.	3837	1	0.24	0.348	532917	0.123
Other plantarflexors	plantarflexion	3507	1	0.38	0.314	481731	0.04
Dorsiflexors	dorsiflexion	1389	0.2	1.01	0.204	221649	0.107

Table 4 : Listing of the equivalent muscles used in our study, their parameters and their action relative to the joints. Note : according to « Gray's Anatomy » p 432, « Hamstrings » is used for biceps femoris, semitendinosus and semimembranosus. According to Hoy, « other plantarflexors » means tibialis posterior, flexor hallucis longus, flexor digitorum longus, peroneus brevis and peroneus longus. « Dorsiflexors » means tibialis anterior, extensor hallucis longus, extensor digitorum longus and peroneus tertius. The muscle activation set corresponds to a bracing situation.

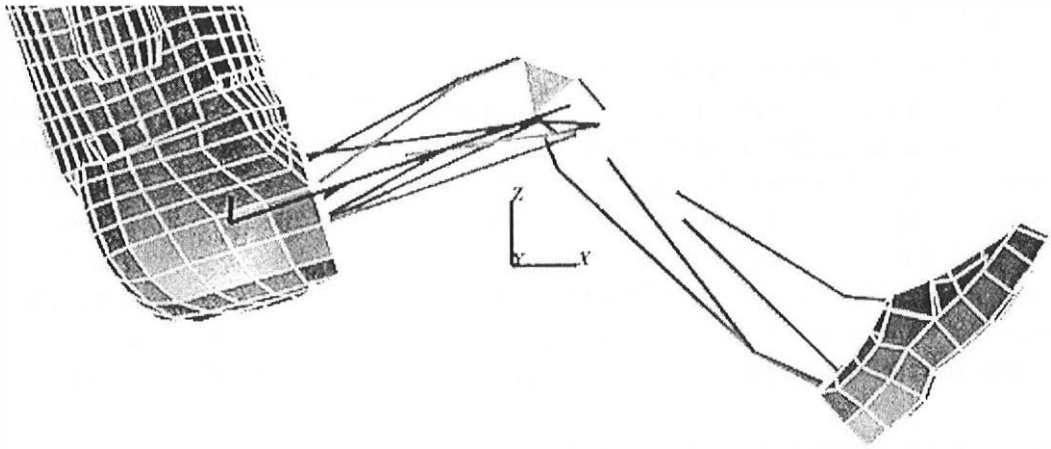

Figure 5 : lower limb musculature model.

RESULTS

Simulations were run to compare the results obtained by the model and those obtained on volunteers by Armstrong [4]. Armstrong performed sled tests where the sled was equipped with a seat, a belt and an instrumented foot rest. One of the sled experimental deceleration pulse is reported in Figure 6.

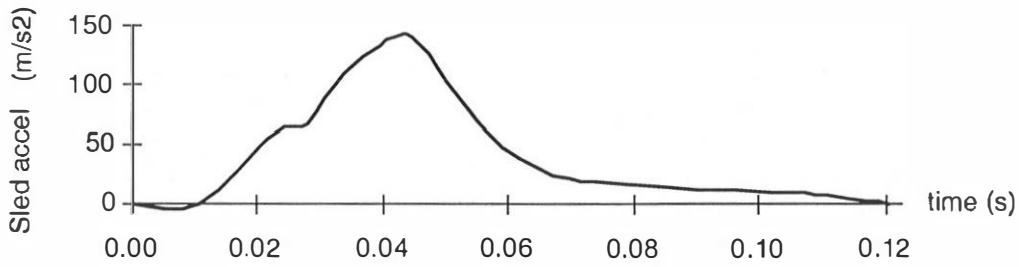

Figure 6 : Sled deceleration in one of the test run by Armstrong.

The model longitudinal force acting at the foot and toe-pan contact was approximately 800 N higher than the experiment results whatever the muscular activation. This was due to a force offset at the pre-crash equilibrium.

The sketch presented in Figure 7 shows a comparison of the standard Hybrid III dummy (with no musculature) and the fully braced model. In case of a moderate severity deceleration pulse (peak = 14 G reached at t=0.04 s), the simulation results showed that the occupant kinematics was greatly modified by muscle tension. Indeed, the standard dummy translated until the seat-belt was tensed (t=0.064 s), then the pelvis rotated around -Y and penetrated the seat cushion. Prior to the crash (t < 0.120 s), the braced model moved rearward due to muscle tension, and during the crash, the knees remained extended and prevented the pelvis from translating. The seat-belt slack was then entirely taken up by the thorax forward movement.

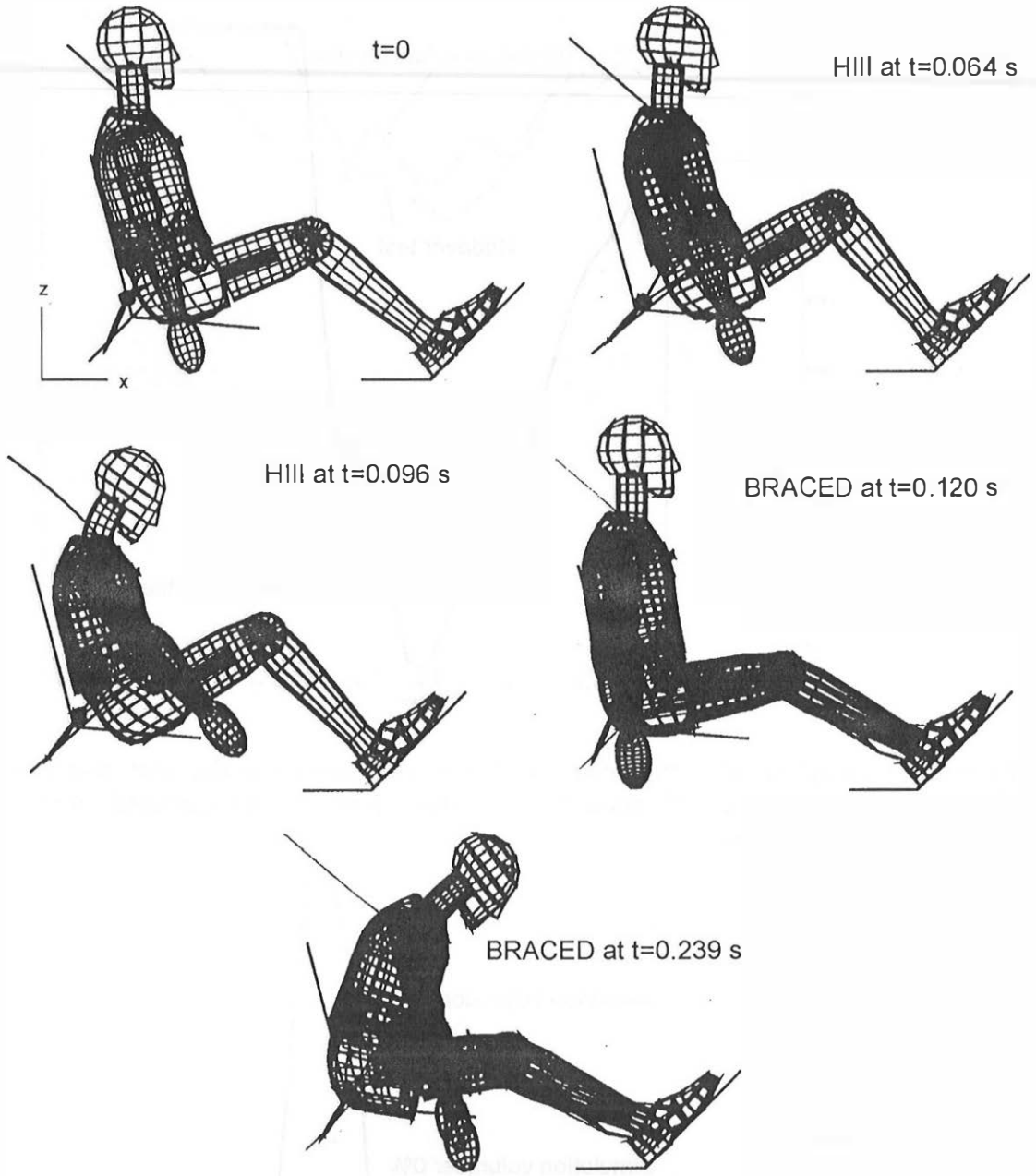

Figure 7 : Kinematic comparison of the standard HIII dummy (no musculature) and the braced model. The initial positions were the same for both. Note: the deceleration pulse is presented in Figure 6, for the braced simulation the pulse was delayed of 0.120 s in order to let the model reach an equilibrium prior to the crash.

The model validation was also conducted using cadaver tests performed by Portier [23]. The cadavers were placed as presented in Figure 10 and a brake pedal, initially in contact with the head of the metatarsals, imposed a dynamic dorsiflexion of the foot. The force acting at the contact between the pedal and the sole of the foot was used to adjust the parameter μ in Equation 3. A comparison between the simulation and test results is presented in Figure 8 and Figure 9. Simulation results for a fully activated volunteer are also plotted.

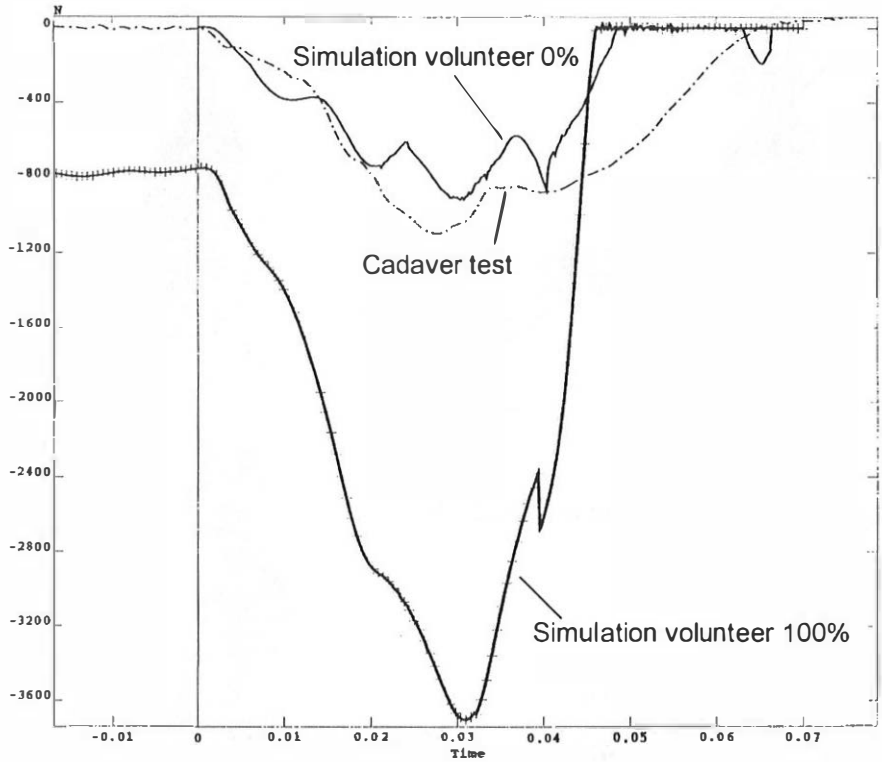

Figure 8 : Longitudinal force acting at the contact between the foot and the pedal. Comparison of the results obtained from a cadaver test and from simulations of 0% and 100% activated volunteers.

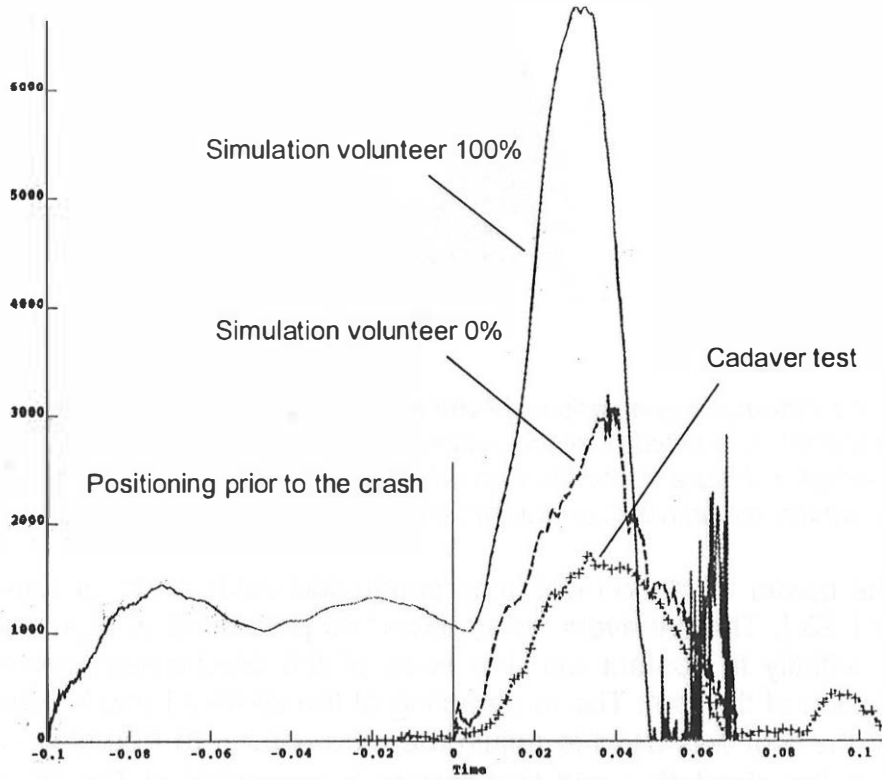

Figure 9 : Tensile force acting in the Achilles tendon. Comparison of the results obtained from a cadaver test and from simulations of 0% and 100% activated volunteers.

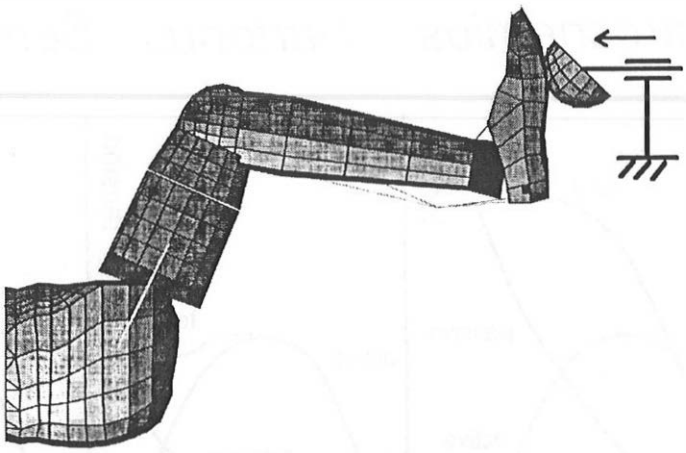

Figure 10 : simulation of the cadaver tests performed by Portier.

According to the simulations performed for the 100% activated volunteer (Figure 8 and Figure 9), the peak forces acting respectively in the Achilles tendon and under the metatarsals are approximately 6500 N and 3700 N. The resultant compressive force acting in the tibia is then approximately 10200 N. From the literature review, such forces are supposed to result neither in Achilles tendon, nor in tibial injuries. Indeed, [10] [19] and [29] reported maximal allowed stress in the Achilles tendon ranging from 91.10^6 Pa to 125.10^6 Pa. If we assume that the Achilles tendon cross section area is 81.10^{-6} m^2 [12], the maximal force to be sustained by the tendon is then ranging from 7371 to 10125 N. [22] reported a maximal compressive force of 10360 N in the tibia.

DISCUSSION

At this stage, the model should be considered as a research tool. Indeed, before accurate predictions could be provided for higher severity, some additional validations and fittings should be performed.

All the simplification assumptions of the study were exposed as clearly as possible. Some of them may be discussed. For example, the isometric passive force was assumed to start for a fiber length equal to the optimal fiber length. Data provided by [30] who investigated several frog muscles do not confirm our assumption (see Figure 11). Indeed, a parameter should be added to describe the fiber length where the passive isometric force starts. However, such data is not available for the 18 equivalent muscles that compose the lower limb musculature. Reasonable simplifications were chosen in order to overcome the lack of biomechanical data.

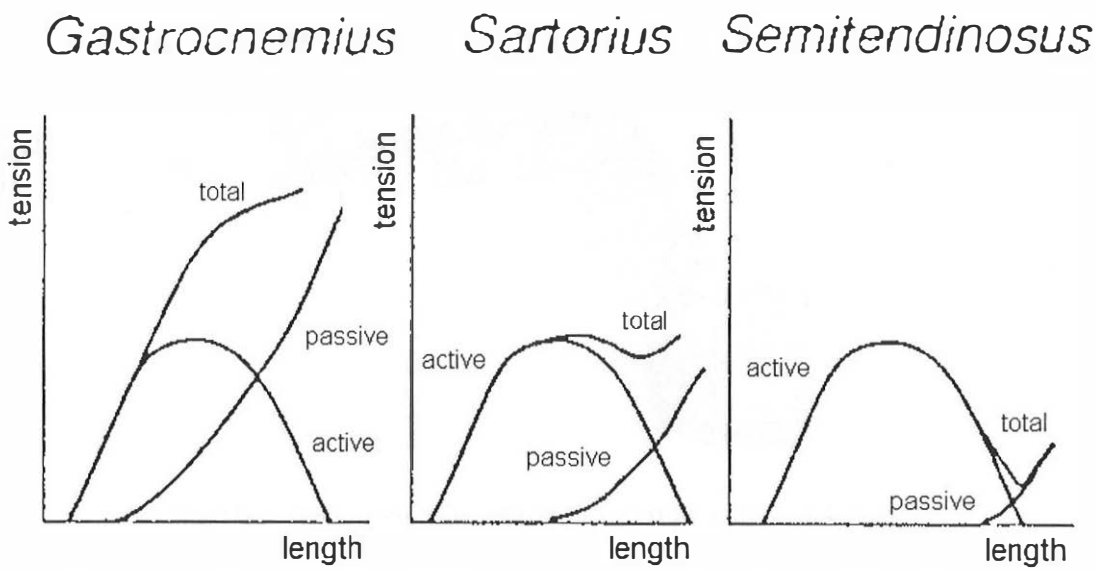

Figure 11 : Example of isometric passive and active force of frog muscles.

In the musculotendon model, the optimal fiber length normalized all the lengths involved in the representation. A sensitiveness study showed this physical parameter had a major influence on the simulation results. An in-depth literature review showed large discrepancies on that point. The lack of consistent biomechanical data is thus of primary importance for further model development.

Moreover, since the skeletal geometry was determined from one cadaver and scaled to correspond to the dummy size, the muscle cross section areas were measured on a second cadaver, the physical properties such as the optimal fiber length were obtained on a third cadaver and finally the muscle paths were determined from anatomy papers and minute in-vivo examinations of a fourth person, the different parameters despite they were individually accurately investigated remain inconsistent. It is then very difficult to assess the global accuracy of the muscle length estimation. Thus, the isometric passive and active forces calculation include this lack of consistency.

This paper is based on an in-depth literature review of lower limb muscle tension modeling. The authors attempted to adapt the information of both musculoskeletal geometry, and musculotendon property modeling, to develop an Hybrid III dummy articulated rigid body model placed in crash-test conditions. It provides a list of assumptions to be made in order to overcome the enormous lack of precise knowledge of the lower limb muscle characteristics. It seems, however, that no model providing accurate predictions can be developed as long as biomechanical data is not available.

CONCLUSIONS

Some priorities clearly appear for the next cadaver investigation studies. Among those priorities, the necessity of consistent musculoskeletal geometry and musculotendon physical properties is widely emphasized.

According to Hoy, the Achilles tension is responsible for approximately 90% of the peak ankle moment. Results reported in the literature shows that during a dynamic dorsiflexion of a cadaver foot [23], the Achilles load can reach 36% of

the tension generated by a trained volunteer during acrobatic jumping [12]. The dynamic strengthening of the triceps surae could thus create a **passive** muscle tension that could reach approximately half of the **active** force acting in the Achilles tendon of an athlete during an acrobatic jump.

The results of the first version model suggests that in a moderate severity crash, muscle tension may significantly modify the occupant kinematics.

The research efforts should keep on evaluating the importance of the lack of muscle tension on the Hybrid III dummy since it is currently used for car regulation.

REFERENCES :

[1] ABBOTT B. C., and WILKIE D. R., « The relation between velocity of shortening and the tension-length curve of skeletal muscle », J Physiol (London), 120, 214, 1953.

[2] AGARWAL, C. G., et GOTTLIEB, G. L., (1977 a) « Oscillation of the human ankle joint in response to applied sinusoidal torque at the foot », J. Physiol., London, 268, 151-176.

[3] ALEXANDER, R., McN, MALOIY G. M. O., KER R. F., JAYES A. S., WARUI C. N., « The role of tendon elasticity in the locomotion of the camel (Camelus dromedarius), J. Zool. (London), 198, 293, 1982.

[4] ARMSTRONG., R. W., WATERS, H. P., and STAPP, J. P. (1968), « Human muscular restraint sled deceleration », Society of Automotive Engineers, SAE No. 680793, in Proc. of the Stapp Conf.

[5] BANDI W., « Chondromalacia patellae und femoro-patelre arthrose. Ätiologie, Klinik und therapie », Helvetica Chir. Acta, Suppl. 11, 1972.

[6] BEGEMAN Paul C., KING A.I., LEVINE R.S., VIANO D.C., "Biodynamic response of the musculoskeletal system to impact acceleration", 24th Stapp Conference Proceedings, pp. 479-509, 1980.

[7] BENNETT, M. B., KER, R. F., DIMERY, N. J., and ALEXANDER, R. McN (1986), « Mechanical properties of various mammalian tendons », J. Zool., Lond. 209, 537-548.

[8] BRAND R., PEDERSEN D., FRIEDERICH J., « The sensitivity of muscle force predictions to changes in physiologic cross-sectional area », J. Biomech., Vol. 19, No 8, pp. 589-596, 1986.

[9] CAVAGNA, G. A., (1970) « Elastic bounce of the body », J. Appl. Physiol., 29, 279-282.

[10] CRONKITE, A. E. (1936) Anat. Rec. 64, 173-186.

[11] GOUBEL, F., (1971) « Relation entre l'EMG intégré et le travail mécanique dans le cas de mouvements effectués à inertie constante, avec ou sans charge », J. Physiol. (Paris) 63, 224.

[12] GRAFE, H. (1969), « Aspekte zur Ätiologie der subcutanen Achillessehnenruptur » Zentralblatt f. Chirurgie 94, 33, 1073-1082.

[13] GROOD E. S., SUNTAY W. J., NOYES F. R., BUTLER D. L., « Biomechanics of the knee-extension exercise », The J. of Bone and Joint Srgery, vol. 66-A, no 5, June 1984.

[14] HERRICK W. C., KINGSBURY H. B., and LOU D. Y. S., « A study of the normal range of strain, strain rate, and stiffness of tendon », J. Biomed. Mater. Res., 12, 877, 1978.

[15] HOY, M. G., ZAJAC, F. E., and GORDON, M. E., (1990) « A musculoskeletal model of the human lower extremity : the effect of muscle, tendon, and moment arm on the moment-angle relationship of musculotendon actuator at the hip, knee, and ankle », J. Biomechanics 23, 2, 157-169.

[16] HUNTER, I. W., and KEARNEY, R. E., (1982) « Dynamics of human ankle stiffness : variation with mean ankle torque », J. Biomechanics, 15, 10, 747-752.

[17] KEARNEY, R. E., and HUNTER, I. W., (1982) « Dynamics of human ankle stiffness : variation with displacement amplitude », J. Biomechanics, 15, 10, 753-756.

[18] KER R. F., DIMERY N. J., and ALEXANDER R. McN., « The role of tendon elasticity in hopping in wallaby (Macropus rufogriseus) », J. Zool. (London), 208, 417, 1986.

[19] KOMI, P. V., (1984) « Biomechanics and neuromuscular performance », Med. Sci. Sports Exerc. 16, 26-28.

[20] LINDAHL O., and MOVIN A., « The mechanics of extension of the knee-joint », Acta Orthop. Scand., 38: 226-234, 1967.

[21] MYERS, B. S., VAN EE, C. A., CAMACHO, D. L. A., WOOLEY, C. T., and BEST, T. M., (1995) « On the structural and material properties of mammalian skeletal muscle and its relevance to human cervical impact dynamics », 39th STAPP Car Crash Conf Proc.

[22] NYQUIST Gerald W., "Injury tolerance characteristics of the adult human lower extremities under static and dynamic loading", SAE Symposium on Biomechanics and Medical Aspects of Lower Limb Injuries, P-186, pp.79-90, San Diego, CA, Oct., 1986.

[23] PORTIER Laurent, 1997 « Sécurité Automobile et Protection des Membres Inférieurs », Thèse de l'Université Paris XII. UFR : Génie Biologique et Médical.

[24] RUGG S. G., GREGOR, R. J., MANDELBAUM, B. R., CHIU, L., (1990) « In vivo moment arm calculations at the ankle using magnetic resonance imaging (MRI) », J. Biomechanics 23, 5, 495-501.

[25] SMIDT G. L., « Biomechanical analysis of knee flexion and extension », J. Biomech., 6, 79-92, 1973.

[26] THOMAS C., personal communication.

[27] WHITE S. C., YACK H. J., WINTER D. A., « A three-dimensional musculoskeletal model for gait analysis. Anatomical variability estimates », J. Biomech., Vol. 22, No 8/9, pp. 885-893, 1989.

[28] WICKIEWICZ T. L., ROY R. R., POWELL P. L. EDGERTON V. R., « Muscle architecture of the human lower limb », Clinical Orthopedics and Related Research, No 179, Oct. 1983, pp275-283.

[29] WILHELM, H. (1975), « Die subcutane Achillessehnenruptur », Unfallheilkunde, 121-330.

[30] WILKIE D. R., (1956) « The mechanical properties of the muscle », Brit. Med. Bull., 12, 177-182.

[31] ZAJAC, F. E., (1989) « Muscle and tendon : properties, models, scaling and appications to biomechanics and motor control », CRC Critical Rev. Biomed. Eng. 17, 359-411.